AD-A056 736 DAVID W TAYLOR NAVAL SHIP RESEARCH AND DEVELOPMENT CE--ETC F/G 13/10
FLARE SLAMMING CHARACTERISTICS OF TWO AIRCRAFT CARRIER BOW CONF--ETC(U)
FEB 78 N K BALES

UNCLASSIFIED DTNSRDC-78-SPD-811-03 NL

1 OF 1
AD A056 736

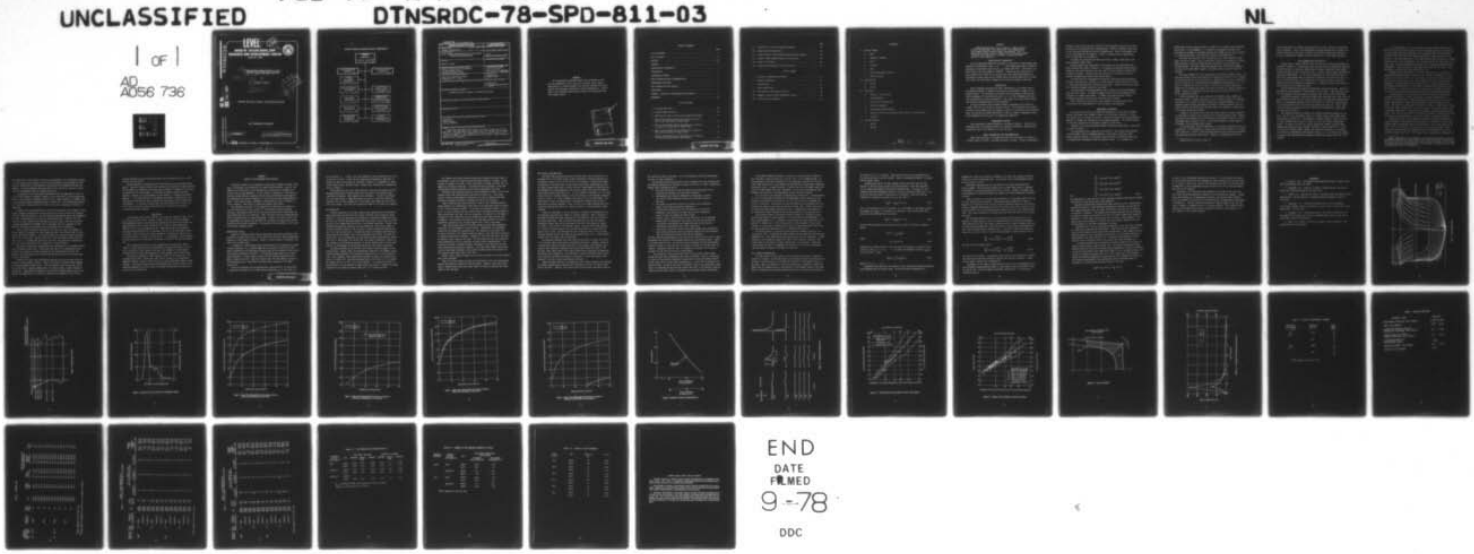

END
DATE FILMED
9-78
DDC

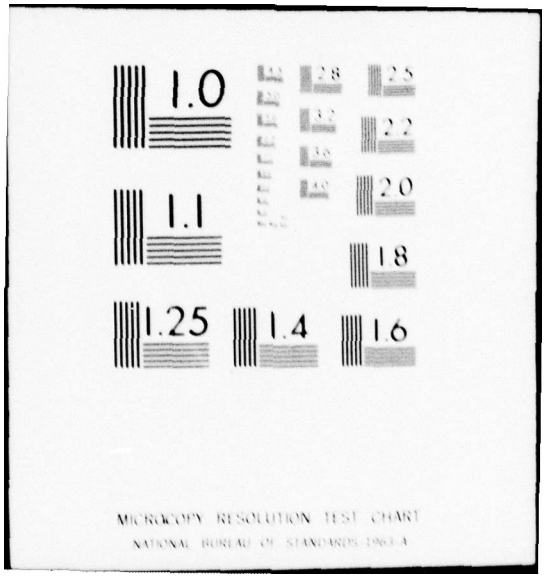
1.0
1.1
1.25
1.4
1.6
2.8
3.2
3.6
4.0
2.5
2.2
2.0
1.8
MICROCOPY RESOLUTION TEST CHART
NATIONAL BUREAU OF STANDARDS 1963-A

LEVEL II

DAVID W. TAYLOR NAVAL SHIP RESEARCH AND DEVELOPMENT CENTER

Bethesda, Md. 20084

FLARE SLAMMING CHARACTERISTICS OF TWO AIRCRAFT CARRIER BOW CONFIGURATIONS

Final rept.

by

Nathan K. Bales

48 p.

APPROVED FOR PUBLIC RELEASE: DISTRIBUTION UNLIMITED

SHIP PERFORMANCE DEPARTMENT

February 1978

DTNSRDC-78-SPD-811-03

FLARE SLAMMING CHARACTERISTIC

MAJOR DTNSRDC ORGANIZATIONAL COMPONENTS

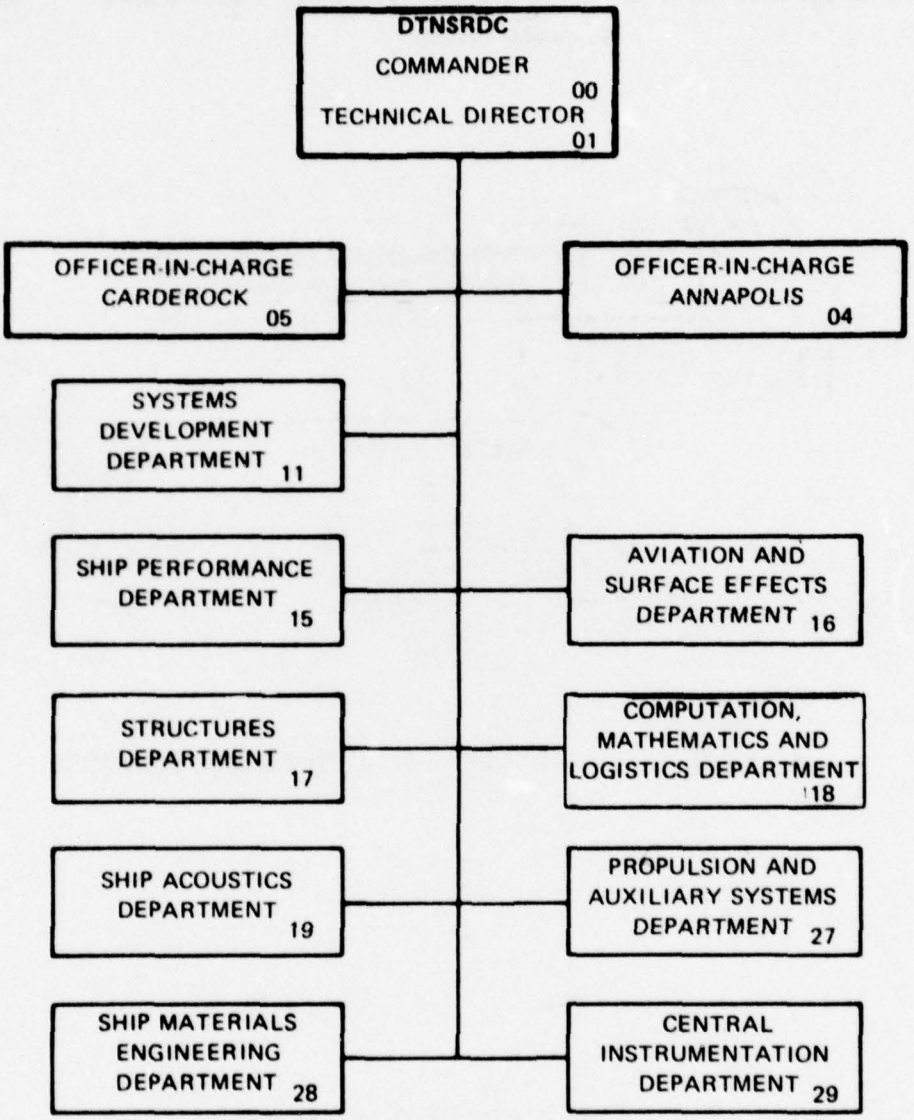

UNCLASSIFIED

SECURITY CLASSIFICATION OF THIS PAGE (When Data Entered)

REPORT DOCUMENTATION PAGE

READ INSTRUCTIONS BEFORE COMPLETING FORM

1. REPORT NUMBER: DTNSRDC 78-SPD-811-03
2. GOVT ACCESSION NO.:
3. RECIPIENT'S CATALOG NUMBER:

4. TITLE (and Subtitle): FLARE SLAMMING CHARACTERISTICS OF TWO AIRCRAFT CARRIER BOW CONFIGURATIONS

5. TYPE OF REPORT & PERIOD COVERED: Final

6. PERFORMING ORG. REPORT NUMBER:

7. AUTHOR(s): Nathan K. Bales

8. CONTRACT OR GRANT NUMBER(s):

9. PERFORMING ORGANIZATION NAME AND ADDRESS:
David W. Taylor Naval Ship Research and Development Center
Bethesda, Maryland 20084

10. PROGRAM ELEMENT, PROJECT, TASK AREA & WORK UNIT NUMBERS:
Project No. 62543
Work Unit Nos. 1-1568-822 & 1-1504-100

11. CONTROLLING OFFICE NAME AND ADDRESS:
Naval Ship Engineering Center
Washington, D.C. 20362

12. REPORT DATE: February 1978

13. NUMBER OF PAGES: 47

14. MONITORING AGENCY NAME & ADDRESS (if different from Controlling Office):

15. SECURITY CLASS. (of this report): UNCLASSIFIED

15a. DECLASSIFICATION/DOWNGRADING SCHEDULE:

16. DISTRIBUTION STATEMENT (of this Report):
APPROVED FOR PUBLIC RELEASE: DISTRIBUTION UNLIMITED

17. DISTRIBUTION STATEMENT (of the abstract entered in Block 20, if different from Report):

18. SUPPLEMENTARY NOTES:

19. KEY WORDS (Continue on reverse side if necessary and identify by block number):
Seakeeping
Flare Slamming
Aircraft Carriers

20. ABSTRACT (Continue on reverse side if necessary and identify by block number):

Seakeeping experiments with a model of a small aircraft carrier are described. Two above-water bow configurations, one V-shaped and one highly flared, are compared. The V-shaped bow is found to pose a lesser risk of structural damage in severe conditions but to be subject to many more small impacts in all conditions.

DD FORM 1 JAN 73 1473 EDITION OF 1 NOV 65 IS OBSOLETE
S/N 0102-LF-014-6601

UNCLASSIFIED
SECURITY CLASSIFICATION OF THIS PAGE (When Data Entered)

FOREWORD

The investigation described herein was performed in 1973, and was documented at that time in an informal report series. Subsequently, it became evident that the data included was rather unique; and therefore, deserving of wider dissemination. Accordingly, this unlimited distribution document was abstracted from the original report.

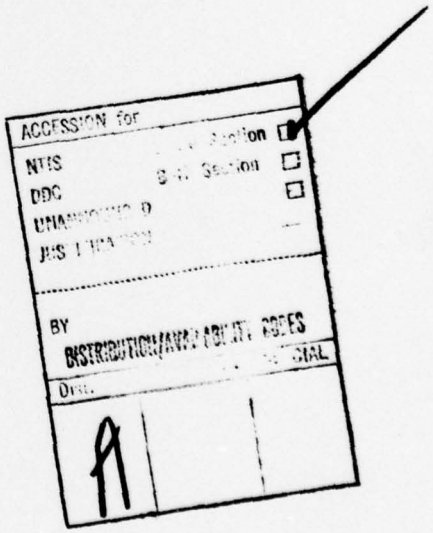

TABLE OF CONTENTS

LIST OF FIGURES

LIST OF TABLES

NOTATION

I. General Symbols

A	Area
C	Geometric constant
F	Force
p	Pressure
t	Time
X	Bow pressure gage location
θ	Vertical slope

II. Superscripts

#1	Bow #1
#2	Bow #2

III. Subscripts

N	Normal to local surface
P	Peak magnitude
S	Stem at 60 foot waterline
V	Vertical component
X	Bow pressure gage location
0	Station 0 at 60 foot waterline with F and p, rise time with t
1	Duration

IV. Special Symbols

V	Bow #1
Y	Bow #2

ABSTRACT

Seakeeping experiments with a model of a small aircraft carrier are described. Two above-water bow configurations, one V-shaped and one highly flared, are compared. The V-shaped bow is found to pose a lesser risk of structural damage in severe conditions but to be subject to many more small impacts in all conditions.

ADMINISTRATIVE INFORMATION

The work described herein was performed by the David W. Taylor Naval Ship Research and Development Center. The Naval Ship Engineering Center funded the experiment and analysis under Work Request Number WR-3-5442. This effort was identified by Work Unit Number 1-1568-822. Preparation and publication of this document were funded by the Conventional Ship Seakeeping Research and Development Program under Project Number 62543 and Block Number SF 43 421 202. This effort was identified by Segment 20 of Work Unit Number 1-1504-100.

INTRODUCTION

Bottom slamming phenomena have been investigated to the extent that it now appears possible to evaluate them during the preliminary stages of the design process. The possibility of similar impact phenomena occurring due to rapid submergence of the above-water bow, i.e., of flare slamming, has been much discussed but sparsely documented. This report is a step toward filling the existing information gap on flare slamming.

The data presented were obtained during an experiment with a model of a small (585 foot or 178 meter) aircraft carrier. Two above-water bow configurations, both asymmetrical with respect to the hull centerline, were evaluated. Thus, the results are highly specialized. They do, however, demonstrate that flare slamming can occur and be of significant magnitude.

EXPERIMENTAL PROGRAM

The experimental program employed is outlined in Table 1. Each bow configuration was to be evaluated under all tabulated conditions. Ballast characteristics were to be identical for the two bows.

MODEL CONSTRUCTION AND INSTRUMENTATION

Model 5297 was built to represent the 585 foot (178 meter) prototype at a linear ratio of 34.412. The model was built to sheer. It was of thin-shell,

mahogany construction; and was fitted with interchangeable bow sections representing the two above-water bow configurations. Figure 1 presents a body plan of the prototype showing the two bow configurations. Box #1 is V-shaped, and will be identified by the symbol V. Bow #2, a highly-flared configuration, will be identified by the symbol Y.

The model was equipped with shaft and struts, rudder, bilge keels, and stock propeller number 4324.

Pressure gages were installed at six locations on the above-water bow. These locations are shown in Figure 2. All gages were mounted flush with and normal to the local surface on the port side of the bow where the flight deck overhang is greater. The port side was chosen on the assumption that the greater overhang would produce more severe impacts.

The model was also instrumented to measure rigid body motions, absolute vertical acceleration at Station 0, and ship-to-wave relative motion at Station 0. Waves were measured well outboard of the model. Motion pictures were taken from a platform rigged outboard of the model.

Time histories of all measurements were recorded on both analog magnetic tape and strip charts. Correlation among the various records generated was afforded by a common time signal. A common time signal was also used to correlate the motion pictures with the strip chart records.

Three channels of electronics, each capable of monitoring the gross statistics of one measurement on a per run basis, were employed.

EXPERIMENTAL PROCEDURE

With each bow attached, the model was ballasted to full scale equivalent design displacement and trimmed in water to an even keel condition. It was then swung in air to obtain its center of gravity location and pitching gyradius. Metacentric height was obtained by an inclining experiment. The natural period of roll was obtained by oscillating the model in calm water.

Complete, full scale equivalent ballast conditions, applicable to both bows, are given in Table 2.

All experiments were conducted in the David W. Taylor Naval Ship Research and Development Center's Seakeeping Basin. This basin is 360 feet (109.7 meters) long by 240 feet (73.2 meters) wide by 20 feet (1.6 meters) deep, and is equipped with wavemakers along two adjacent sides. It is spanned by a

bridge which can be rotated through a 45 degree arc to admit various headings with respect to the wavemakers. A carriage to accommodate personnel and experimental equipment is suspended beneath the bridge, and can run its length at a preselected speed. For additional details, see Reference 1.*

The model was attached to the carriage only by a slack umbilical cable bundle and safety ropes. Thus, it was free to move in all degrees of freedom. Model propeller revolutions were manually controlled to match model and carriage speeds. The model rudder was automatically controlled by feedback of sway and yaw measurement signals to maintain lateral position under the carriage.

Existing programs were used to generate the required irregular waves. The selected programs produce wave energy over frequencies from 0.2 to 1.4 radians per second at the scale of the prototype. Maximum energy occurs at frequencies close to those of the corresponding Pierson-Moskowitz wave spectra, i.e., at about 0.4 radians per second for waves of 30 foot (9.1 meter) significant height and 0.5 radians per second for waves of 20 foot (6.1 meter) significant height. Figure 3 illustrates the spectrum used for waves of 30 foot (9.1 meter) significant height.

As the experiment was to be conducted in irregular waves, samples of sufficient length to admit derivation of valid statistics had to be obtained. The duration of a single run down the basin is usually inadequate. So, the standard irregular wave experimental procedure of making repeated runs in a given condition and effectively splicing these runs together to obtain sufficient sample length was followed.

A sample of 20 minutes full scale equivalent length is usually regarded as sufficient to obtain valid statistics for vertical-plane motions. However, the statistical stability of the above-water bow pressures critical to this experiment was not known a priori. It was thus decided to obtain samples of 30 minutes full scale equivalent length.

As the experiment involved comparison of alternative above-water bow configurations, it was necessary to ensure that each bow was subject to the same wave conditions. Ideally, this would mean ensuring that each bow experienced the same wave encounter time history. However, accomplishing this with a

---

*References are listed on page 19.

free-running model in irregular waves would be, at best, difficult and prohibitively expensive. Hence, the experimental procedure employed was to ensure statistical identity of the waves to which the alternative bows were subjected. This was accomplished through run-by-run monitoring of wave height statistics.

DATA PRESENTATION AND ANALYSIS

General data on sample lengths, wave statistics and monitored responses are presented in Table 3. It should be noted that the pairs of experiments comparing alternative bows at identical combinations of nominal significant wave height, relative heading and ship speed agree well in terms of sample length and measured significant wave height. It can also be observed that the alternative above-water bow configurations had no consistent influence on the gross statistics of pitch or relative motion. The similarity of the relative motion statistics indicates that the incidence of wetness due to shipping of green water would be nearly equal for the alternative bows.

The bow pressure data required a moderately extensive analysis. Details of the analysis are presented in the Appendix to this report. Here the basic data will be presented, and the analysis procedures and results will be described.

Preliminary analysis of the bow pressure data indicated that those pressures measured below the 60 foot (18.3 meter) waterline were relatively insignificant. Hence, the subsequent analysis effort was focussed on the three pressure gages located along the 60 foot (18.3 meter) waterline (see Figure 2). Basic impact pressure statistics derived from the time histories generated by these gages are presented in Table 4.

The tabulated statistics exhibit one striking difference between the two bows: Bow #1 (V) is invariably subject to several times as many small impact pressures as is Bow #2 (Y). With respect to heavier impacts, there is little to choose between the two bows in waves of 20 foot (6.1 meter) significant height. In waves of 30 foot (9.1 meter) significant height, notably higher maximum peak pressures were recorded on Bow #2 (y) than on Bow #1 (V). Even in 30 foot (9.1 meter) waves, though, the distinction between the two bows is not obvious at intermediate peak pressure levels, e.g., in terms of the number of impacts with peak pressures exceeding 30 pounds per square inch (20.7×10^4 pascals).

It is hypothesized that the large number of small impacts registered on Bow #1 (V) is due to water piling up on its extremely blunt stem. The motion pictures taken during the experiment tend to substantiate this hyposthesis. For Bow #1 (V), they show very frequent generation of heavy spray in way of the stem. Such spray generation occurs even when the ship is subject to rather moderate levels of bow submergence. By contrast, Box #2 (Y), which has a much finer stem, is seen to generate heavy spray only in instances of extreme bow submergence. The implication is that Bow #2 (Y) would be less prone to deck wetness due to blown spray than would Bow #1 (V).

Determining the significance of the fact that Bow #2 (Y) is subject to higher maximum peak pressures than Bow #1 (V) requires consideration of the response of the hull structure to the loadings occasioned by these pressures. Both the bow plating and the hull girder responses of the prototype were so considered. Dynamics effects were accounted for in accord with Reference 2. The extreme value statistics of the impact pressures were evaluated in accord with Reference 3. Requisite structural properties were obtained from References 4 and 5 and from data supplied by the Naval Ship Engineering Center.

The significance of the bow pressure data with respect to bow plating response was evaluated in terms of the risk of plastic deformation as a function of operating time. Risk analyses were performed only for the most severe combinations of significant wave height, relative heading and ship speed. The results are presented in Figures 4 through 7. Each figure compares the risk of plastic deformation for the two bows at a specified location and a specified combination of significant wave height, relative heading and ship speed. Only the stem and Station 0 locations are shown, as the data available for Station 2 was inadequate to support the analysis techniques employed.

Numerical levels of risk indicated by Figures 4 through 7 are subject to some uncertainty. The pressure level necessary to occasion the onset of bow plating plastic deformation was only established to lie in the range from 96 (66.2×10^4) to 139 (95.8×10^4) pounds per square inch (pascals). Risk curves were derived under the assumption that an intermediate value of 118 pounds per square inch (81.4×10^4 pascals) would cause plastic deformation.*

---

*After this analysis was performed, a more definitive pressure criterion, described in Reference 6, was brought to the author's attention. Application of this criterion to the present case yields a limiting pressure of 114 pounds per square inch (78.6×10^4 pascals). On this basis, it appears that the risk curves presented here are slightly low.

The sensitivity of the level of risk to this assumption is illustrated by Figure 8. This figure gives risk as a function of the pressure limit assumed to cause plastic deformation for 100 minutes of operation in the highest-risk case examined. It can be observed that the level of risk varies by a factor of three over the established range of limiting pressures.

Irrespective of the uncertainty associated with the magnitude of risk, it is felt that Figures 4 through 7 present a fair comparison of the proposed bows. Thus, in the conditions examined, Bow #2 (Y) is usually subject to a higher risk of bow plating plastic deformation than is Bow #1 (V). The differences involved are nontrivial: usually factors of three to five and occasionally an order of magnitude.

Evaluation of the significance of the bow pressure data with respect to hull girder response requires that the vertical force acting on the bow be computed from the measured pressures. The bow pressure measurements taken were inadequate to admit a high degree of accuracy in such computations. However, the time history of total vertical force acting on the port side of the bow can be very crudely approximated by assuming that a specified vertical component of each measured pressure acts uniformly over an assigned area of influence.

This procedure indicates that Bow #1 (V) would, at least for moderate to severe impacts, be subject to lesser peak vertical forces than Bow #2 (Y) even given equal peak pressures. It has been shown that the peak pressures acting on Bow #1 (V) are, in fact, usually equal to or less than those acting on Bow #2 (Y). Thus, it followed that Bow #1 (V) will as a rule experience lesser peak vertical forces than Bow #2 (Y) in moderate to severe impacts.

Detailed vertical force computations were performed for an extremely severe event recorded on each bow. It was found that Bow #2 (Y) experienced a peak vertical force about 2.5 times as great as that experienced by Bow #1 (V). Further, the time histories of the vertical forces acting on the two bows were found to be similar.

Similarity of the force time histories implies that the two bows would be subject to equal dynamic effects. Hence, hull girder responses should compare in the same manner as peak forces. For the extreme events considered, Bow #2 (Y) would induce a hogging moment about 2.5 times as large as that induced by Bow #1 (V). Taken about the midship, these induced bending moments would be of significant magnitude as the forces in question act primarily in way of the

forward perpendicular and can exceed seven tons per square foot (15.4×10^6 pascals) for Bow #2 (Y).

Another approach to evaluating the forces acting on the alternative bows exists. Heavy bow impacts distort the recorded bow acceleration time histories, and the degree of distortion introduced can be taken as a measure of the force occasioned by the causal impact. An attempt was made to perform such an analysis. However, the accelerometer proved subject to ringing during heavy impacts. It was thus difficult to ascertain the levels of distortion to be attributed to the impacts, and no definitive conclusions could be drawn from the analysis. It can only be noted that distortion levels of 6 (1.8) to 12 (3.7) feet per second in each second (meters per second in each second) occurred during heavy impacts.

CONCLUSIONS

In extremely severe events, Bow #1 (V) is overtly superior to Bow #2 (Y) by virtue of the fact that it poses a lesser threat of structural damage. During moderate events, the distinction between the two bows is blurred; but some preference must be given to Bow #1 (V) in that it would experience smaller vertical forces than Bow #2 (Y). When mild events are considered, the trend favoring Bow #1 (V) is reversed. Bow #1 (V) is invariably subject to several times as many small impact pressures (10 pounds per square inch, 6.9×10^2 pascals, or less) as is Bow #2 (Y). In consequence, the likelihood of deck wetness due to blown spray is greater for Bow #1 (V) than for Bow #2 (Y).

The foregoing conclusions can be summarized by stating that, where a clear-cut choice between the two proposed bow configurations exists, Bow #1 (V) is preferred in all respects save one: the incidence of small impact pressures and the associated likelihood of deck wetness due to blown spray.

The greater incidence of small impacts on Bow #1 (V) may be due to its extremely blunt stem. Given this, some virtue is seen in a configuration generally similar to Bow #1 (V); but with its upper waterlines drawn to finer endings. Care should be exercised in developing such lines as fining of the waterline endings will tend to fine the forward sections and thus give rise to the vices of Bow #2 (Y).

APPENDIX

DETAILS OF BOW PRESSURE DATA ANALYSIS

The basic problem to be considered is structural response to impact loadings. Accordingly, the possibility of dynamic effects exists. That is, the response of a structure to such loadings can differ from its response to a static load of equal magnitude. In the context of Reference 2, evaluation of possible dynamic effects requires that the time characteristics and shape of the loading and the natural frequency of the structure under investigation be known. Given these factors, Reference 2 determines the ratio of dynamic to static response. This ratio is termed the dynamic load factor.

The subsequent sections of this appendix will describe the analysis of the bow pressure data in the context of the foregoing problem statement. Initially, the general nature of the bow pressure data will be described; and some definitions will be introduced. Then, the data reduction scheme employed will be described and its results presented. Finally, the prior results will be synthesized to evaluate the influence of the measured pressures on the bow plating and hull girder responses. All quantities will be given in full scale units unless otherwise noted.

DESCRIPTION OF DATA

Figure A-1 exhibits three "events" abstracted from the bow pressure time histories recorded on Bow #1 (V) in bow seas of 30 foot (9.1 meter) significant height at a ship speed of 20 knots. Event A is mild, Event B is moderate, and Event C is a severe case.

In Figure A-1, each pressure gage is identified by its vertical and longitudinal positions, e.g., pressure gage 60-S is located on the 60 foot (18.3 meter) waterline at the stem while pressure gage 55-3 is located on the 55 foot (16.8 meter) waterline at Station 3. The indicated gage zeros are at atmospheric pressure. A water contact causes the time history generated by the gage to depart from zero. When the contact ends, the time history returns to the established zero. Thus Event B involved water contacts on all gages except 55-3.

Each zero departure can be quantitatively characterized, as illustrated for gage 60-S in Event B, by a peak pressure magnitude, p_p, a rise time, t_0,

and a duration, t_1. Further, each zero departure can be qualitatively characterized by its shape. Thus, the zero departures exhibited by gage 60-S in Figure A-1 might be described as "rounded" in Event A, "triangular" in Event B, and "blast pulse" (having a sharp, linear rise, followed by an exponential decay) in Event C.

Zero departures with rise times obviously less than one-fourth the minimum anticipated wave encounter period (on the order of two seconds) were classified as impacts. Only impacts were considered. In Event A of Figure A-1, the time history of gage 60-S shows the end of a long zero departure (possibly due to water running off of the flight deck) which was not classified as an impact. All other zero departures shown in the figure are impacts.

DATA REDUCTION

Initial inspection of the bow pressure data indicated that the measurements taken below the 60 foot (18.3 meter) waterline were relatively insignificant. Under any given operating condition, the pressure gages below the 60 foot (18.3 meter) waterline registered at most half as many impacts as did the more active gages along the 60 foot (18.3 meter) waterline. Further, the maximum peak pressures registered by the sub-60 foot (18.3 meter) gages in any given condition were at most one-third of those registered along the 60 foot (18.3 meter) waterline. (In absolute terms, the highest peak pressures measured below the 60 foot (18.3 meter) waterline were around 15 pounds per square inch, 10.3×10^4 pascals, as contrasted to nearly 90 pounds per square inch, 62.1×10^4 pascals, on the 60 foot, 18.3 meter, waterline.) Hence, it was decided to limit detailed analysis of the bow pressure data to that measured by the three gages located along the 60 foot (18.3 meter) waterline.

Focusing attention on the 60 foot (18.3 meter) waterline gages, it was observed that, in many cases, the preponderant majority of the impacts registered had peak pressures of 10 pounds per square inch (6.9×10^4 pascals) or less. Most commonly, these impacts were rounded in shape (as illustrated by Event A in Figure A-1); and had peak pressures on the order of 3 to 5 pounds per square inch (2.1×10^4 to 3.4×10^4 pascals). To expedite the data reduction effort, it was decided to simply count the number of impacts with peak pressures of 10 pounds per square inch (6.9×10^4 pascals) or less.

For impacts with peak pressures exceeding 10 pounds per square inch, it was decided to read rise time, duration and peak pressure. Further, it was decided to classify the shape of each such impact as being of either the triangular or the blast pulse type. Consideration was also given to the time relationships between pressures at the various measurement locations.

Resultant peak pressure statistics were presented in Table 4 of the text. Pressure pulse time characteristics are given in Table A-1. This table applies across all experimental conditions, but only to impacts with peak pressures exceeding 10 pounds per square inch (6.9×10^4 pascals).

Shape classification proved difficult. Many of the recorded pressure pulses seemed to be transitional cases which could have been placed in either of the a priori selected classes. A few were of nondescript shape. At any rate, it can be observed that the heavier impacts recorded were invariably of blast pulse shape, and that, with one exception, the majority of the impacts recorded for each combination of bow configuration and gage location were triangular. The exception occurred for the stem gage on Bow #2 (Y) where a significant majority of the recorded impacts had a blast pulse shape.

Time relationships among the recorded pressure pulses were remarkably consistent for all moderate to severe events. Independent of experimental conditions (including bow configuration), the tendency in such event was for only the 60 foot (18.3 meter) waterline gages at the stem and at Station 0 to register significant pressures. Pressure at the stem rose first, but that at Station 0 had a shorter rise time. The end result was that the peak pressures registered at the two locations occurred nearly simultaneously. The pressure at Station 0 decayed rapidly, returning to zero while the stem was still experiencing significant pressure. Even when small impacts were registered at other gage locations, they usually occurred within the duration of the pressure pulse registered at the stem.

Events B and C shown in Figure A-1 are fairly typical of the time relationships just described.

Many of the mild events recorded also conformed to the time relationship pattern described for moderate to severe events. However, there were exceptions. Notable among these were those events in which no pressure was registered by the stem gage.

BOW PLATING CONSIDERATIONS

The Naval Ship Engineering Center specified that the bow plating of the prototype was to be 0.5625 inches (1.439 centimeters) thick and supported by stiffeners spaced 2.5 by 4.0 feet (0.76 by 1.22 meters). Computations based on Reference 4 indicated that a steel plate having these dimensions and with its edges clamped would have a natural period of approximately 0.00625 seconds. The minimum rise times measured on the bow were almost five times as large as this natural period (see Table A-1). In the context of Reference 2, it is thus evident that the loadings imposed on the bow plating by the measured pressures would be static, i.e., that a dynamic load factor of one is applicable. The implication is that the magnitudes of the measured pressures are directly indicative of plating response. Thus, the fact that higher maximum peak pressures were measured on Bow #2 (Y) would be subject to proportionately higher response.

Given the foregoing, it was of interest to determine the significance of the measured pressures with respect to plating response. Hence, Clarkson's Allowable Pressure Criterion, Reference 5, was applied to the bow plating as previously specified. This procedure indicated that the onset of plastic deformation would occur due to pressures in the 96 to 135 pound per square inch (66.2×10^4 to 95.8×10^4 pascals) range. Here the lower limit applies to a plate of infinite aspect ratio and the upper limit to a plate with an aspect ratio of one. The plating will have an aspect ratio of 1.6, so some limiting pressure within the computed range should apply to it. Unfortunately, though, only the range could be determined.

All measured pressures were less than the 96 pound per square inch (66.2×10^4 oascals) lower limit given by Clarkson's Criterion. However, pressures of almost 90 pounds per square inch (62.1×10^4 pascals) were measured, so it appeared that pressures exceeding the 96 pound per square inch (66.2×10^4 pascals) limit might easily arise under statistically identical circumstances. To explore this possibility, it was decided to apply the extreme value statistical analysis procedures developed in Reference 3 to the bow pressure data measured in the most severe experimental condition.

There was some difficulty in selecting a most severe condition for analysis. The highest maximum peak pressures were recorded in 30 foot (9.1 meter) head seas at 20 knots. However, more rather high pressures were recorded in 30 foot

(9.1 meter) bow seas at 20 knots. So it was decided to perform the analysis for both of these conditions.

The analysis procedure employed for each combination of bow configuration and heading considered (at 20 knots in waves of 30 foot, 9.1 meter, significant height) was an enumerated below.

1. The first 30 minutes of the bow pressure data obtained for the condition was divided into two-minute intervals.
2. The maximum peak pressure registered by each gage on the 60 foot (18.3 meter) waterline during each two-minute interval was read.
3. The maxima so read were plotted on extreme value probability paper in the manner outlined by Reference 3.
4. A theoretical distribution line was defined in accord with Reference 3 and drawn on the same extreme value probability paper on which the maxima had been plotted.
5. Control curves, within which at least 68 percent of the observed maxima would be expected to fall given that they were drawn from a population statisfying the assumptions made in deriving the theoretical distribution line, were constructed.
6. The control curves were drawn on the same extreme value probability paper used previously, and the agreement between the plotted maxima and the theoretical distribution line was examined.

The data from the measurements at the stem and at Station 0 were found to agree reasonably well with the corresponding theoretical distribution lines. Figure A-2 shows a typical case. No results could be obtained from the measurements taken at Station 2 on the 60 foot (18.3 meter) waterline as the data were too limited. Subsequent material will, accordingly, be devoted to the results obtained for the stem and Station 0 measurements.

The probability levels associated with a given pressure level varied widely with both bow configuration and relative heading. This is illustrated by Table A-2 which gives probability levels read from the theoretical distribution lines for all cases under consideration. It can also be inferred from Table A-2 that, in some of the cases considered, there is an appreciable probability of exceeding the 96 pound per square inch (66.2×10^4 pascals) pressure found to be the lower limit for the onset of bow plating plastic deformation.

The extreme pressures analyzed to produce the results given in Table A-2 were typically caused by waves 35 to 45 feet (10.7 to 13.7 meters) high. As the experimental procedures employed for the experiment assured only that the lower order statistics of wave height were reproduced for experiments comparing alternative bows, it seemed desirable to demonstrate that the higher order statistics of wave height were also comparable. To this end, the measured wave heights were analyzed in the same manner as were the bow pressures.

The results of this analysis are summarized in Figure A-3. Plotted maxima for the four experiments involved are distinguished by point shape, but the theoretical distribution line and the control curves shown are averages over the four conditions. Individually fitted distribution lines differed from the average line shown by less than two percent in mean value. Hence, the results of the extreme wave height analysis are held to substantiate the validity of bow comparison results obtained from the like analysis of the pressure data.

The extreme pressure distribution shown in Figure A-2 includes a return period scale along its upper boundary. The return period corresponding to a given peak pressure, e.g., 10 minutes for 50 pounds per square inch (34.5×10^4 pascals) in Figure A-2, is the time required--on the average--for that peak pressure to be exceeded. Return period can be included here because each pressure datum used was representative of a constant time interval.

The return period of a specified peak pressure provides a basis for calculating the risk of exceeding the peak pressure during arbitrary time intervals (Reference 3). Such computations were performed for the bow pressures. A peak pressure of 118 pounds per square inch (81.4×10^4 pascals), central to the range found for the onset of plastic deformation, was specified. Resultant curves giving the risk of exceeding this pressure as a function of operating time were given in Figures 4 through 7 of the text.

HULL GIRDER CONSIDERATIONS

The first mode vertical period of the prototype hull girder is approximately 0.71 seconds. As has been noted, all pressures acting on the bow during moderate to severe events occur within the duration of the pressure pulse at the stem. Thus, the duration of the force induced by a moderate to severe bow impact will be roughly equal to the duration of the pressure pulse of the stem. Table A-1 indicates that pressure pulse durations at the stem are typically on

the order of 0.7 to 1.3 seconds. These durations are in the neighborhood of the natural period of the hull girder. Hence, considering Reference 2, dynamic effects appear likely.

Assessing the nature of these dynamic effects requires that the time history of vertical force acting on the bow be known. Such time histories can be crudely approximated from the bow pressure data. Let $P_{NX}(t)$ be the pressure time history measured normal to the local surface at location X. Let θ_X be the vertical slope of the surface at location X. Then the vertical component of pressure at location X is on the order of

$$P_{VX}(t) = P_{NX}(t) \cos \theta_X \tag{A-1}$$

Now, let an effective area of influence, A_X, be assigned to each gage location; and assume that $P_{NX}(t)$ is constant over this area. Then the vertical force acting on the specified area is given by

$$F_{VX}(t) = A_X P_{NX}(t) \cos \theta_X \tag{A-2}$$

and the total vertical force acting on the port side of the bow is approximately

$$F_V(t) = \sum_X C_X P_{NX}(t) \tag{A-3}$$

where

$$C_X = A_X \cos \theta_X \tag{A-4}$$

Equation (A-3) holds for all t, and can thus be evaluated at a series of discrete t's, say t_i, i = 1, 2, ..., M, given the measured values of $P_{NX}(t_i)$ for all X and i. Thus,

$$F_V(t_i) = \sum_X C_X P_{NX}(t_i) \tag{A-5}$$

where i = 1, 2, . . ., M.

Equations (A-3) and (A-5) are limited to port side forces because pressures were measured only on the port side. As the bow under investigation is

asymmetrical, total force cannot be assumed to be twice that acting on the port side even in long crested head seas. In bow seas, such an approximation would be even further in error.

Additional complications are introduced by the sparse distribution of pressure gages. This situation requires that a rather large area of influence be assigned to the pressure measured at each location. However, the gage locations employed do effectively bound the regions over which significant pressures occurred.

Table A-3 gives the vertical slope parameters for each gage location on the two bow configurations evaluated. Considering these parameters in light of Equation (A-1) indicates that, even given equal measured pressures, the vertical pressure component experienced by Bow #1 (V) would be less than or equal to that acting on Bow #2 (Y) at each gage location above the 50 foot (15.2 meter) waterline. This trend reverses for the gage locations along the 50 foot (15.2 meter) waterline.

The preceding description of the bow pressure data indicates that, for moderate to severe impacts, only the stem and Station 0 pressure measurements taken along the 60 foot (18.3 meter) waterline were of major relevance, and that the peak pressures measured at these locations occurred nearly simultaneously. Thus, the preceding results indicate that at the instant when these peak pressures occur, the port side of the bow will experience a peak vertical force of

$$F_{VP}^{\#1} = 0.65\, A_S^{\#1}\, p_{PS}^{\#1} + 0.79\, A_O^{\#1}\, p_{PO}^{\#1} \qquad \text{(A-6)}$$

with Bow #1 (V) attached; and of

$$F_{VP}^{\#2} = 0.65\, A_S^{\#2}\, p_{PS}^{\#2} + 0.91\, A_O^{\#2}\, p_{PO}^{\#2} \qquad \text{(A-7)}$$

with Bow #2 (Y) attached. In Equations (A-6) and (A-7) the subscript S implies the stem location and the subscript 0 implies the Station 0 location. Superscript numbers indicate bow configuration.

Assignment of the areas in Equations (A-6) and (A-7) is problematical, but any consistent scheme employed tends to yield larger areas for Bow #2 (Y) than for Bow #1 (V). One such scheme is sketched in Figure A-4. It yields the following results:

$$A_S^{\#1} = 156 \text{ feet}^2 \ (14.5 \text{ meter}^2)$$

$$A_S^{\#2} = 200 \text{ feet}^2 \ (18.6 \text{ meter}^2)$$

$$A_O^{\#1} = 175 \text{ feet}^2 \ (16.3 \text{ meter}^2)$$

and

$$A_O^{\#2} = 341 \text{ feet}^2 \ (31.7 \text{ meter}^2) \qquad \text{(A-8)}$$

The implication is that Bow #2 (Y) will experience greater peak vertical forces than Bow #1 (V) even given equal peak pressures.

Detailed vertical force computations were carried out for a severe event recorded on each bow. Peak pressures registered at Station 0 on the 60 foot (18.3 meter) waterline were, in light of Equations (A-6) and (A-7), taken as a criterion of severity. The maximum peak pressure measured at this location occurred at 20 knots in bow seas of 30 foot (9.1 meter) significant height for both bows. In each case, the selected event involved a high pressure at the stem as well as at Station 0 on the 60 foot (18.3 meter) waterline but very little pressure at the other measurement locations.

Equation (A-5), with C_X as defined by Equations (A-4) and (A-8) and Table A-3, was used to perform the computations. Time intervals were selected to suit the local nature of the event under consideration. They ranged from 0.01 seconds during the rise time phase of each event to 0.50 seconds during the decay phase of the event on Bow #1 (V). Resultant time histories of total vertical force on the port bow for both events are given in Figure A-5.

It can be observed that the peak force acting on Bow #2 (Y) is about 2.5 times as high as that acting on Bow #1 (V). This large discrepancy results primarily from the fact that the peak pressure measured at Station 0 on Bow #2 (Y) was twice as high as that measured on Bow #1 (V) at the same location (71.1 versus 35.7 pounds per square inch, 49.0×10^4 versus 24.6×10^4 pascals). Though the absolute magnitudes of peak vertical force exhibited by Figure A-5 are rendered questionable by the assumptions made in defining areas of influence, the implied peak vertical force per unit area,

$$F_{PV}/A = p_{PS} \cos \theta_S + p_{PO} \cos \theta_O \qquad \text{(A-9)}$$

is felt to be of reasonable quantitative accuracy. In this restricted context, it can be noted that Bow #2 (Y) experiences a peak vertical force per unit area of 7.2 tons per square foot (111.2×10^6 pascals) as a result of the event under consideration. The corresponding figure for Bow #1 (V) is 4.5 tons per square foot (69.5×10^6 pascals).

Exclusive of the long decay phase exhibited by the Bow #1 (V) case, the force time histories exhibited by Figure A-5 are qualitatively similar. Though their decay phases are of exponential character, the initial rates of decay which they exhibit are much faster than indicated by the exponential decay model in Reference 2. The most applicable Reference 2 model appears to be, for both cases, a simple, triangular pulse of 0.3 second duration. This being the case, each bow force shown would produce a dynamic load factor on the order of 1.1 with respect to hull girder response.

REFERENCES

1. Brownell, W.F., "A Rotating Arm and Maneuvering Basin," David Taylor Model Basin Report 1053 (Jul 1956).

2. Frankland, J.M., "Effects of Impact on Simple Elastic Structures," David Taylor Model Basin Report 481 (Apr 1942).

3. Gumbel, E.J., "Statistical Theory of Extreme Values and Some Practical Applications," National Bureau of Standards Applied Mathematics Series 33 (Feb 1954).

4. Greenspon, J.E., "Stresses and Deflections in Flat Rectangular Plates Under Dynamic Lateral Loads Based on Linear Theory," David Taylor Model Basin Report 774 (Apr 1955).

5. Greenspon, J.E., "An Approximation to the Plastic Deformation of a Rectangular Plate Under Static Load with Design Applications," David Taylor Model Basin Report 940 (Jun 1955).

6. Wood, R.H., "Plastic and Elastic Design of Slabs and Plates," The Roland Press, New York (1961).

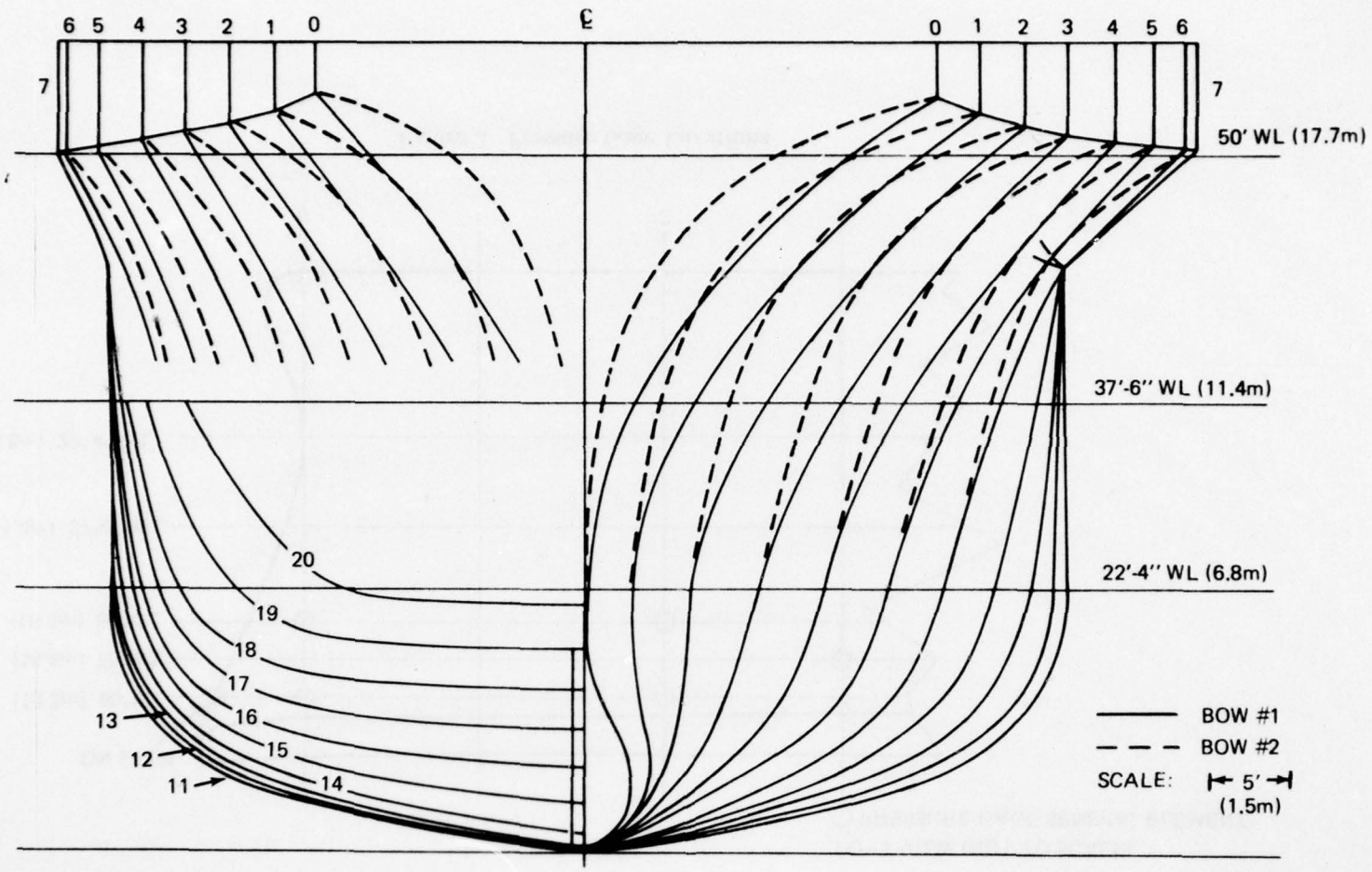

Figure 1 Prototype Body Plan

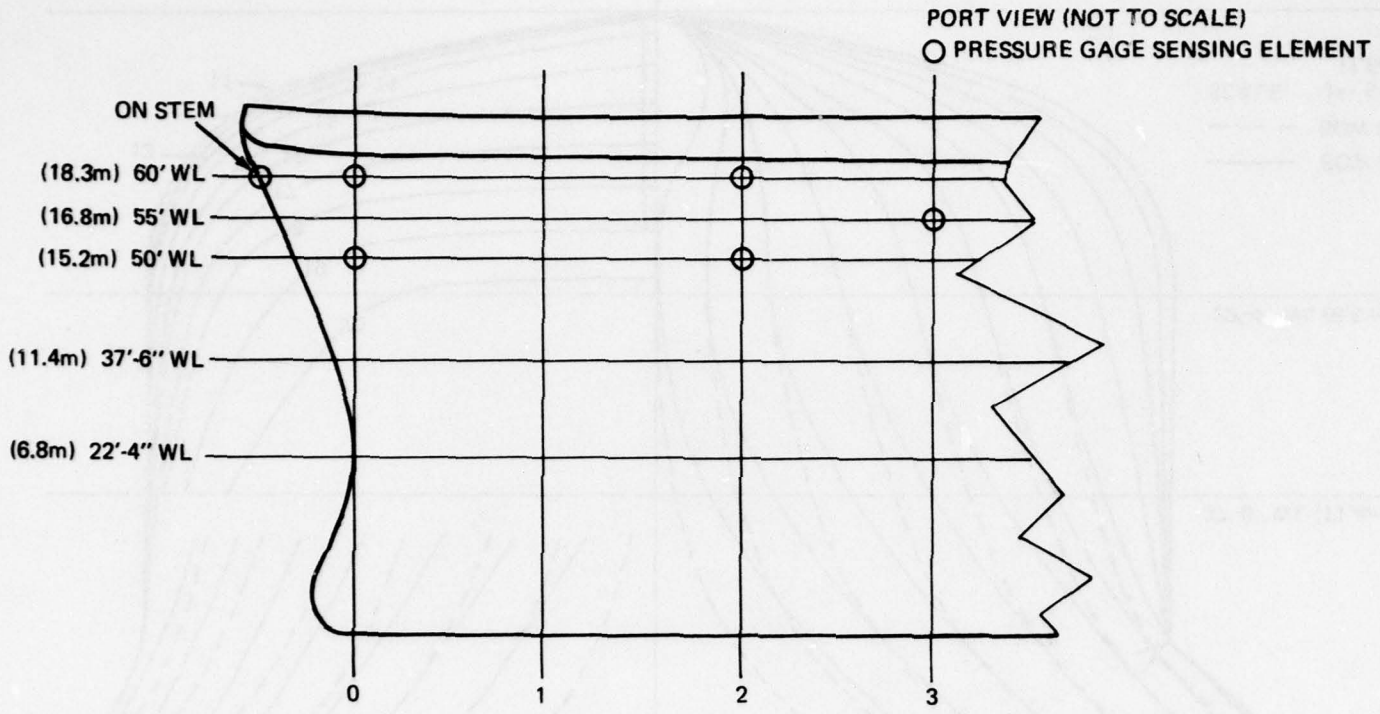

Figure 2 Pressure Gage Locations

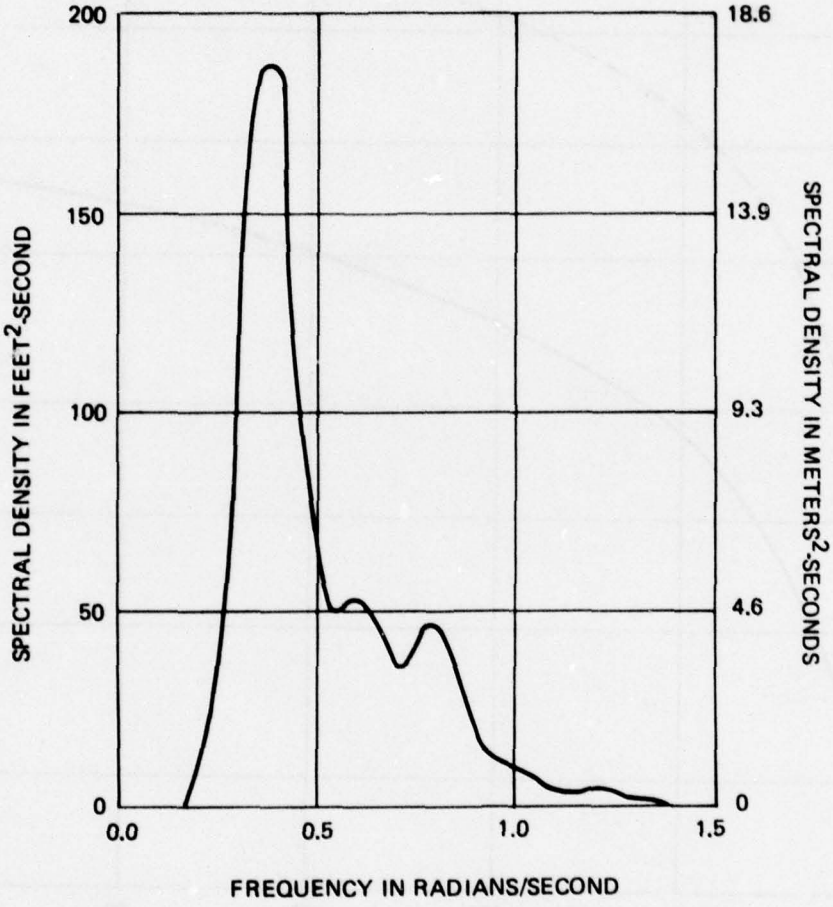

Figure 3 Spectrum for Waves of Thirty Foot Significant Height

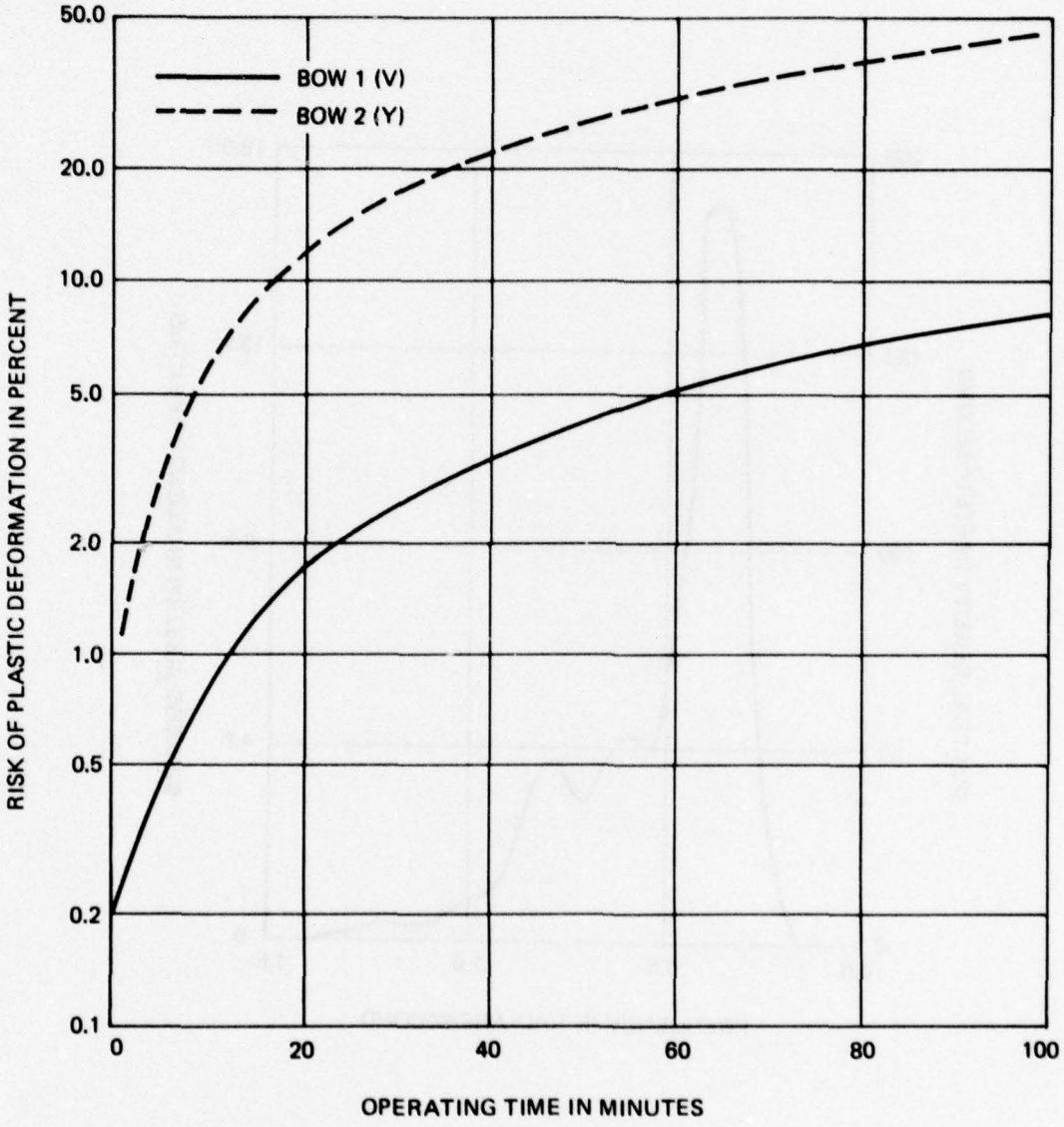

Figure 4 Risk of Bow Plating Plastic Deformation at Stem in Thirty Foot Head Seas at Twenty Knots

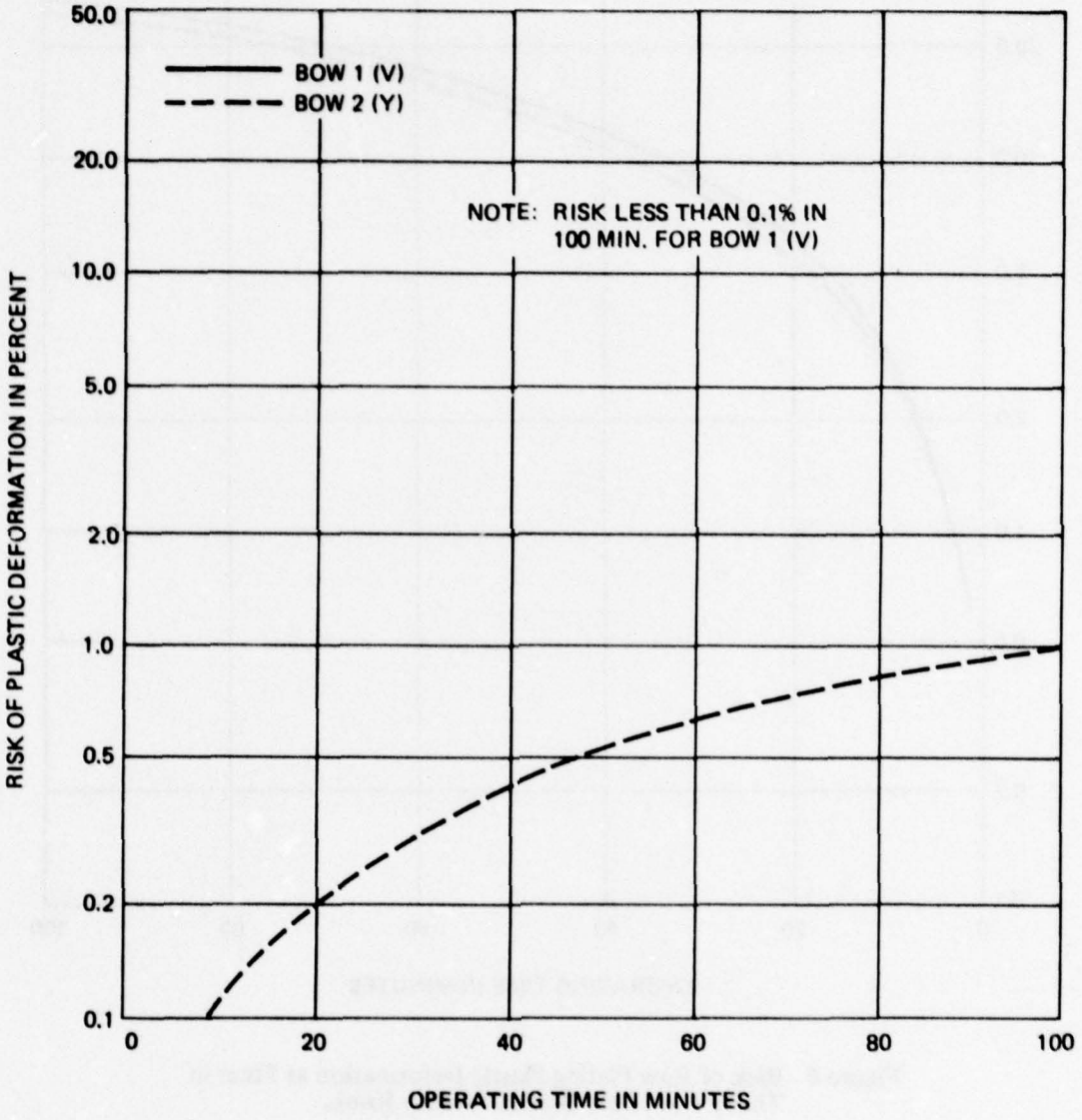

Figure 5 Risk of Bow Plating Plastic Deformation at Station 0 in Thirty Foot Head Seas at Twenty Knots

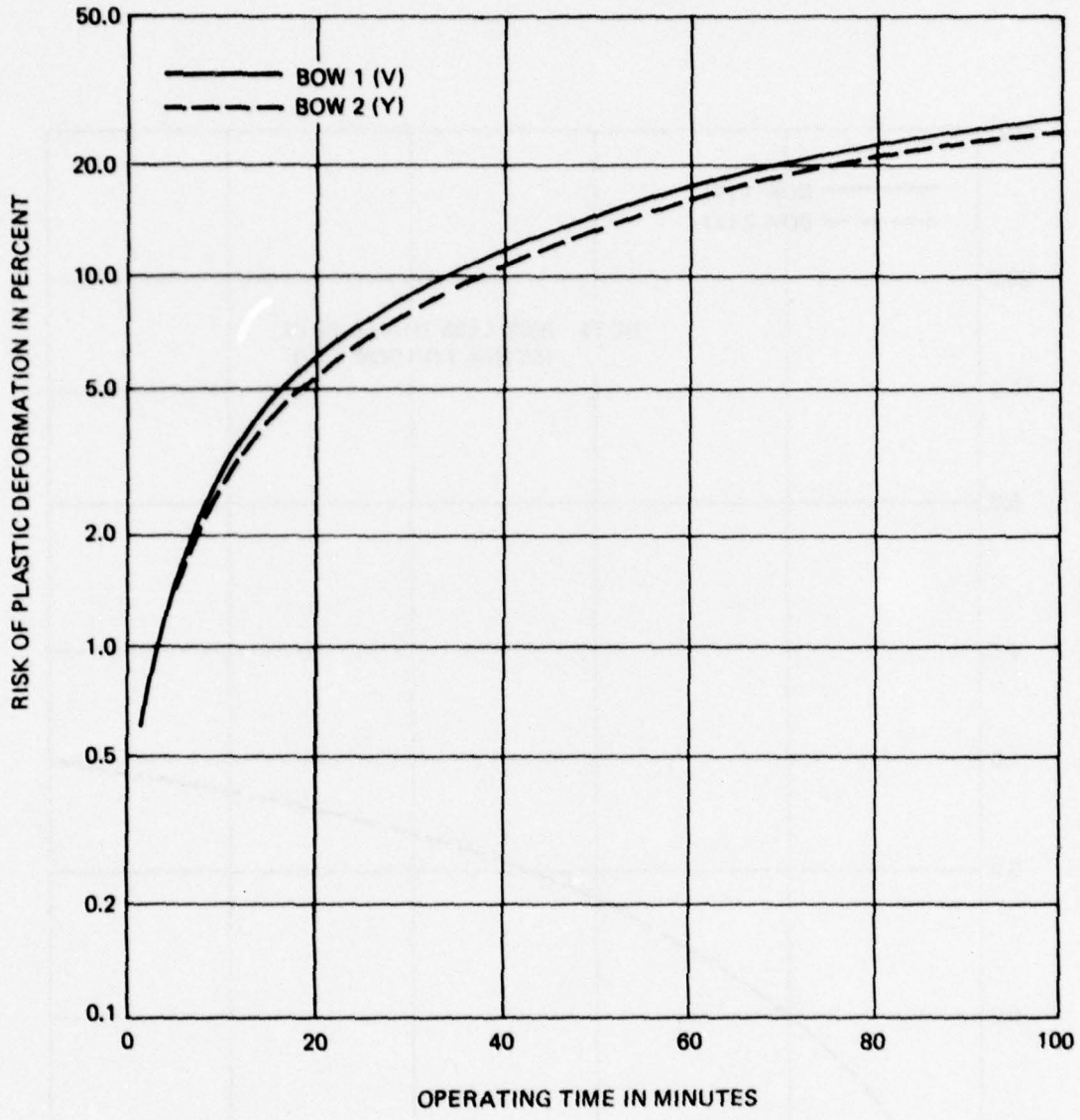

Figure 6 Risk of Bow Plating Plastic Deformation at Stem in Thirty Foot Bow Seas at Twenty Knots

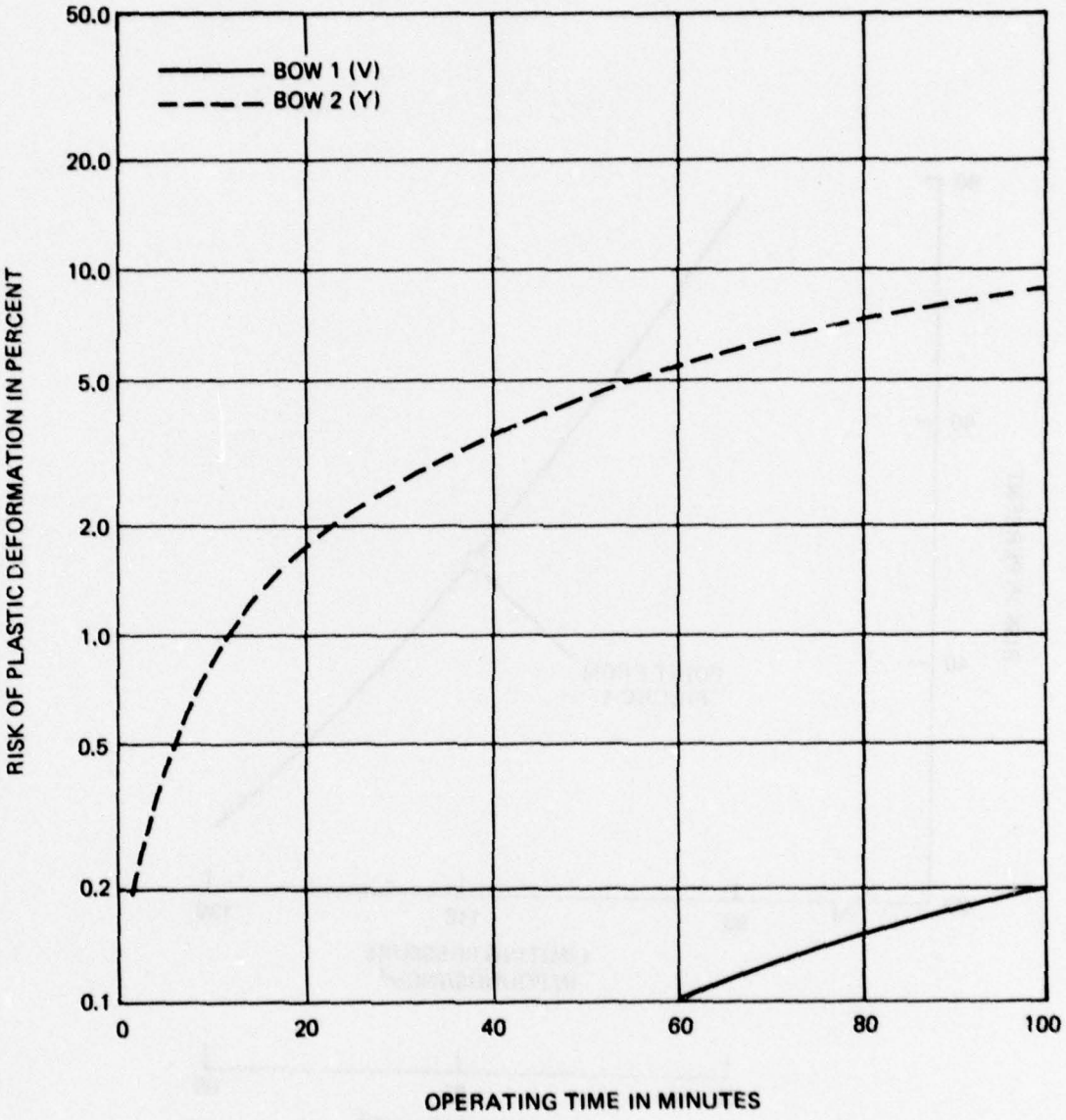

Figure 7 Risk of Bow Plating Plastic Deformation at Station 0 in Thirty Foot Bow Seas at Twenty Knots

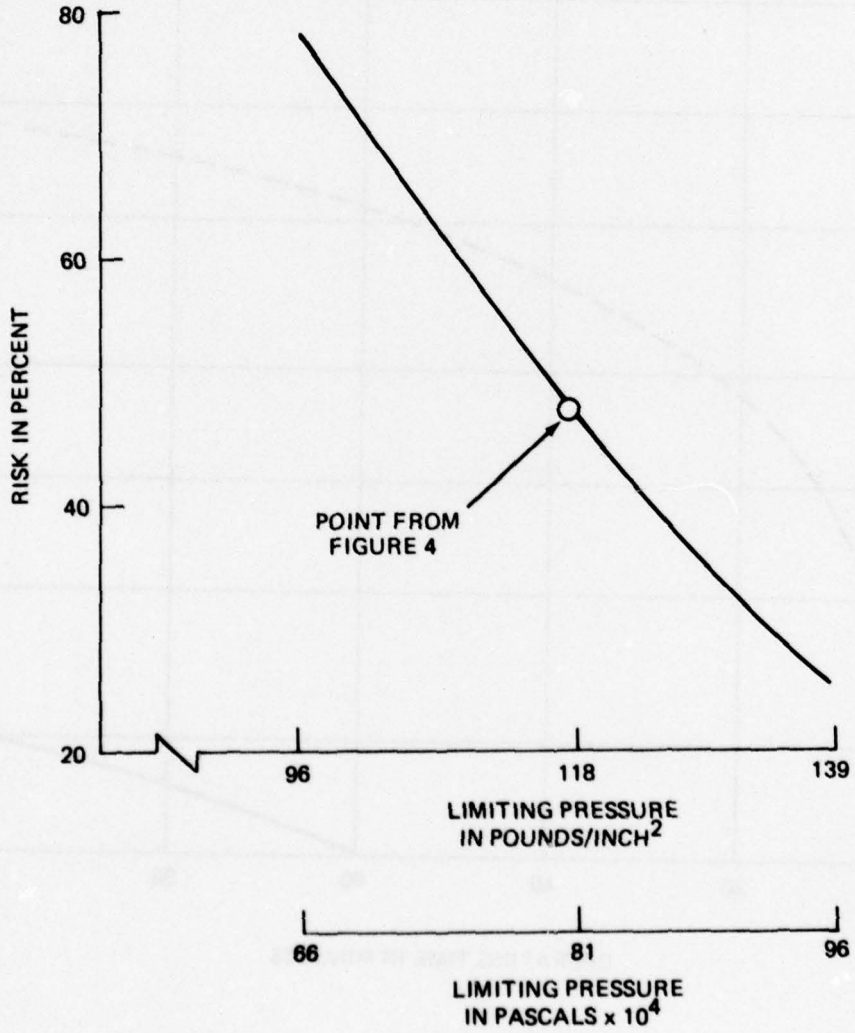

Figure 8 Sensitivity of Risk to Limiting Pressure

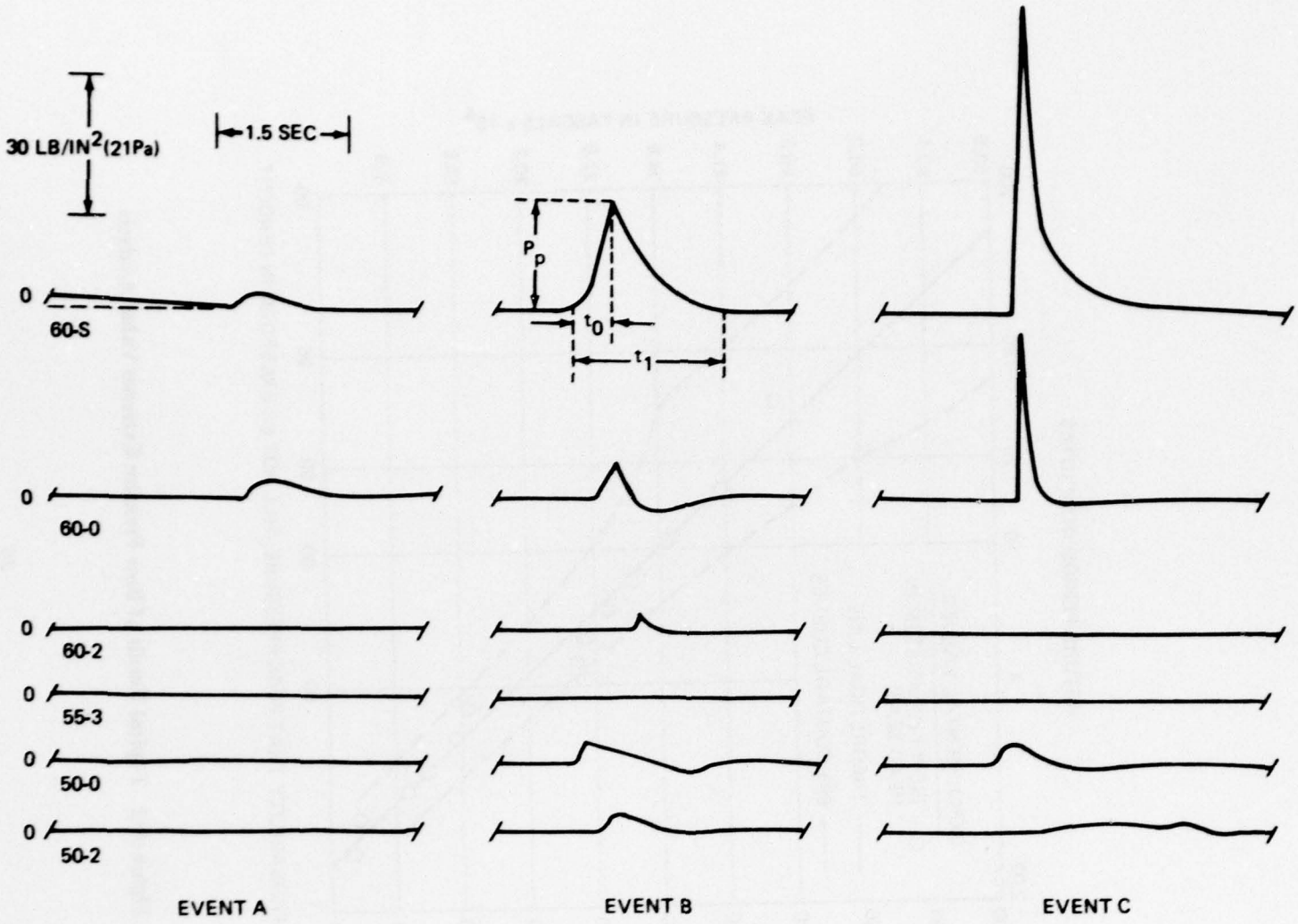

Figure A-1 Sample Bow Pressure Events

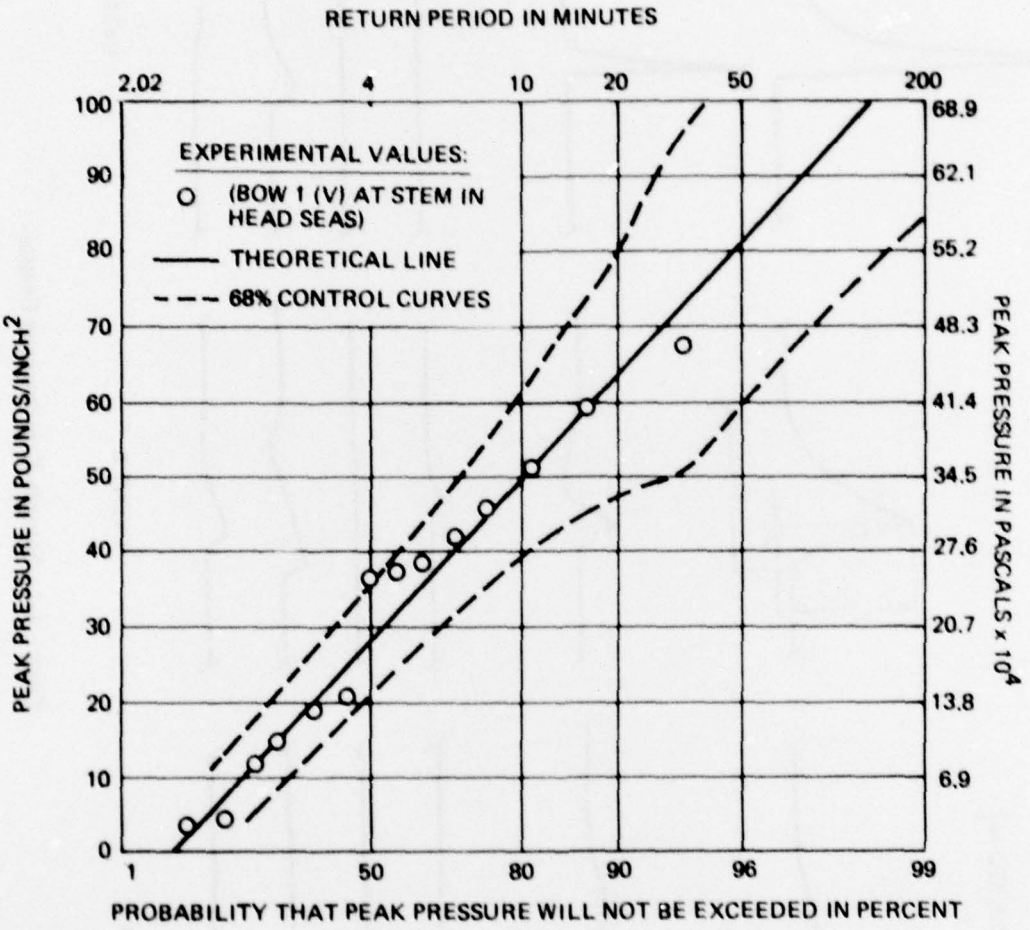

Figure A-2 Typical Result of Bow Pressure Extreme Value Analysis

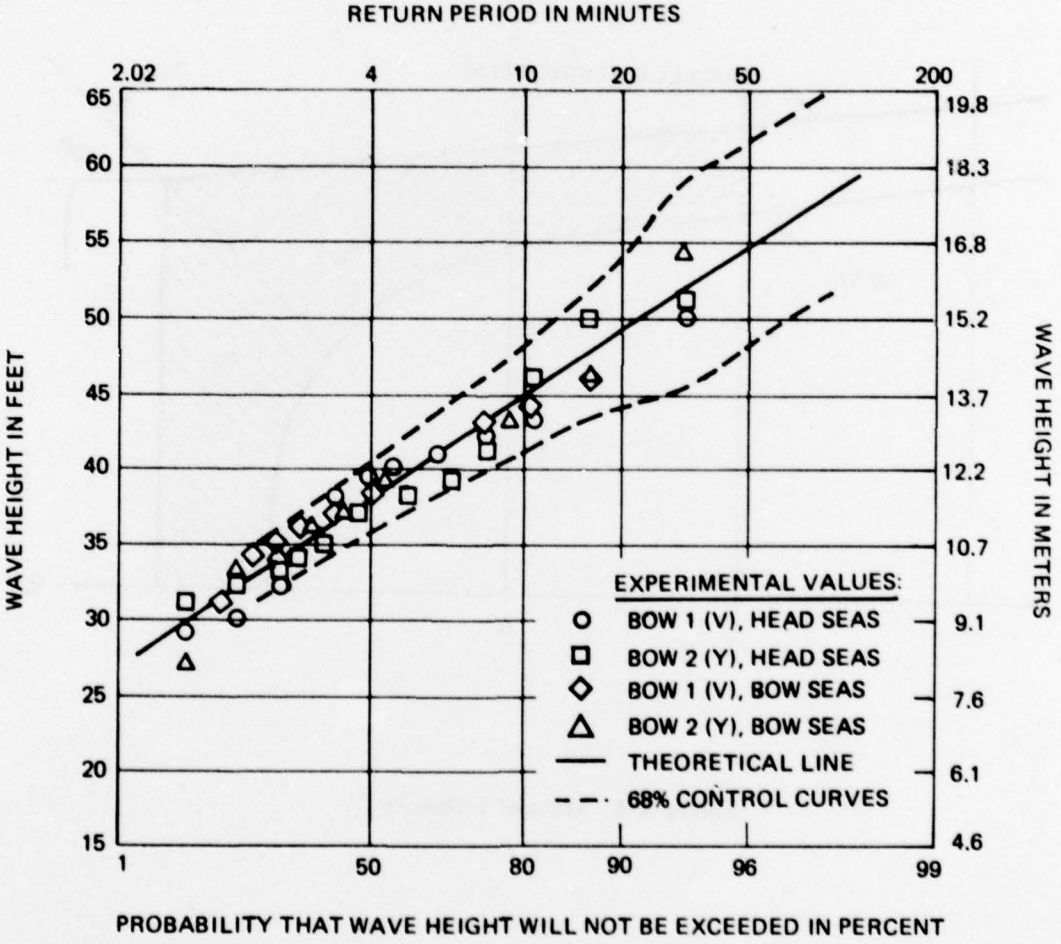

Figure A-3 Results of Wave Height Extreme Value Analysis

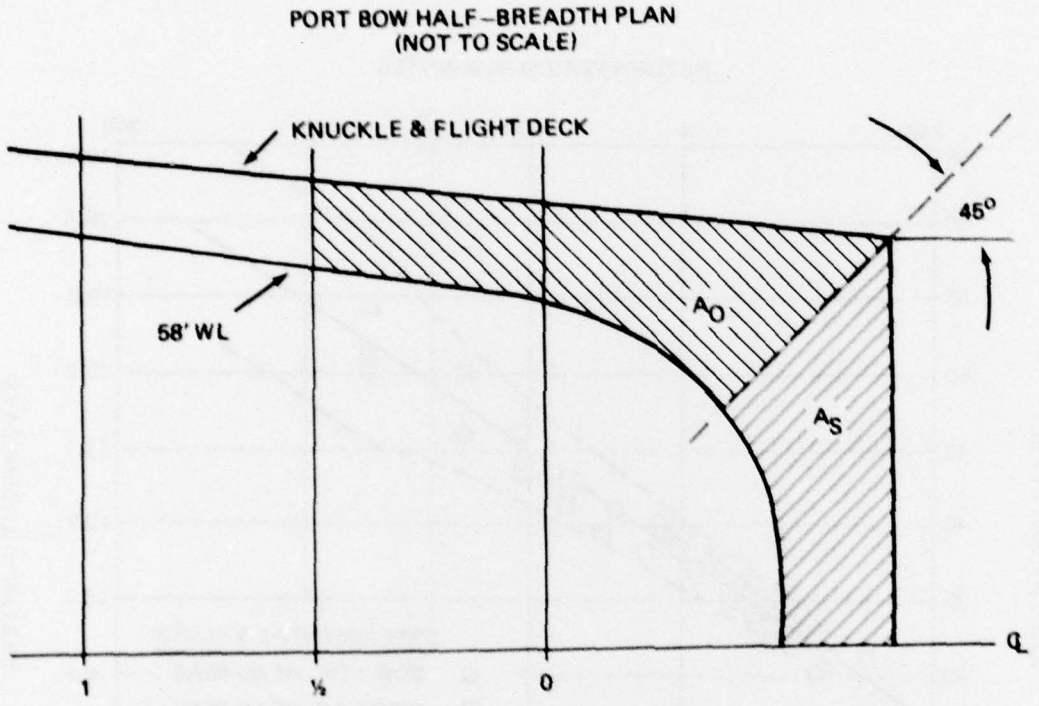

Figure A-4 Areas of Influence

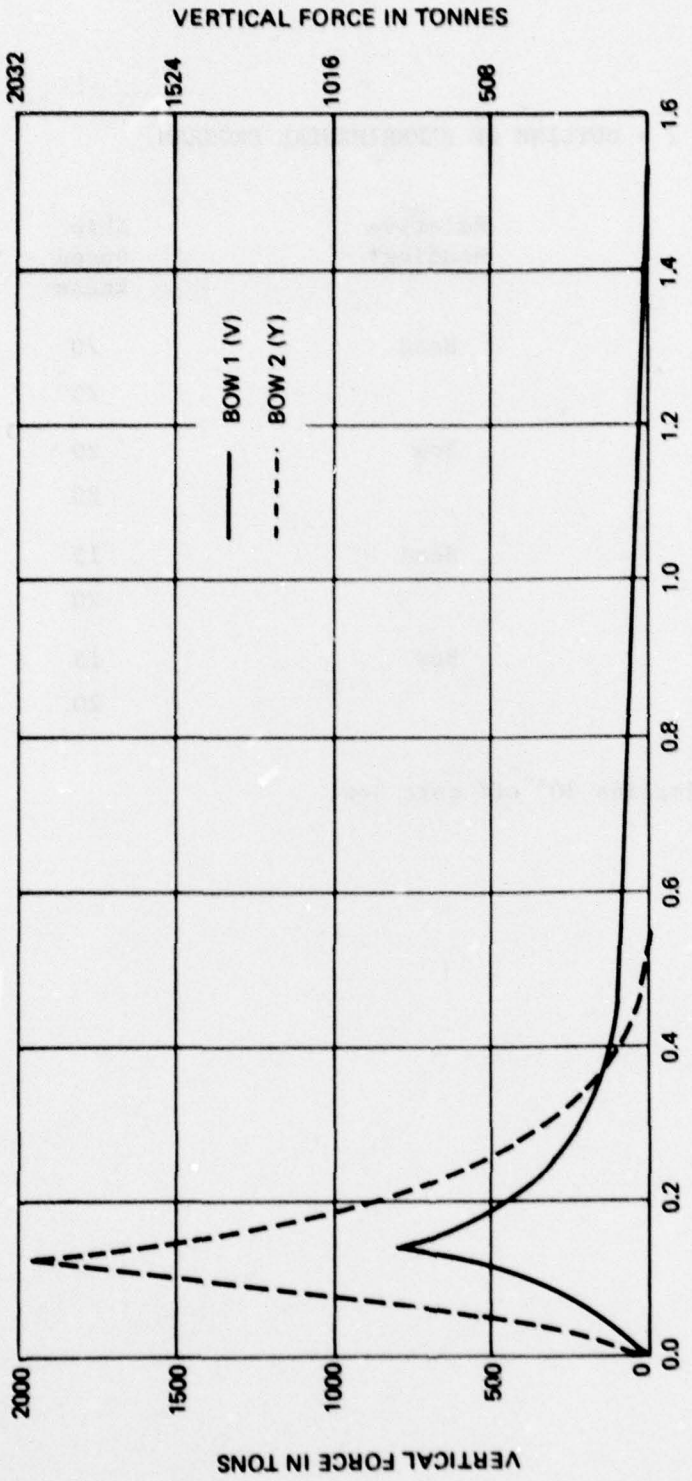

Figure A-5 Computed Time Histories of Vertical Force

TABLE 1 - OUTLINE OF EXPERIMENTAL PROGRAM

Significant Wave Height ft (m)	Relative Heading*	Ship Speed knots
20 (6.1)	Head	20
		25
	Bow	20
		25
30 (9.1)	Head	15
		20
	Bow	15
		20

*"Bow" implies 30° off port bow.

TABLE 2 - BALLAST CONDITIONS

Parameter, Units	Magnitude
Displacement, salt water tons (tonnes)	14,100 (14,326)
Draft, feet (meters)	22.09 (6.73)
Longitudinal Center of Buoyancy Distance aft of Midship, feet (meters)	18.3 (5.58)
Vertical Center of Gravity Distance above Keel, feet (meters)	32.0 (9.75)
Longitudinal Radius of Gyration/Ship Length	0.250
Metacentric Height, feet (meters)	10.9 (3.32)
Period of Roll (seconds)	11.68

TABLE 3 - GENERAL DATA

Nominal Significant Wave Height ft	(m)	Relative Heading*	Ship Speed knots	Bow	Sample Length min	Measured Significant Double Amplitude Wave Height ft	(m)	Relative Motion ft**	(m)	Pitch deg
20	(6.1)	Head	20	#1(V)	30.4	20	(6.1)	45	(13.7)	5.4
				#2(Y)	30.2	20	(6.1)	45	(13.7)	5.6
			25	#1(V)	30.7	21	(6.4)	50	(15.2)	5.5
				#2(Y)	31.0	20	(6.1)	50	(15.2)	5.7
		Bow	20	#1(V)	30.5	20	(6.1)	48	(14.6)	5.6
				#2(Y)	29.4	21	(6.4)	46	(14.0)	5.6
			25	#1(V)	29.9	21	(6.4)	56	(17.1)	5.9
				#2(Y)	29.4	21	(6.4)	54	(16.5)	5.7
30	(9.1)	Head	15	#1(V)	31.6	30	(9.1)	55	(16.8)	8.1
				#2(Y)	32.1	30	(9.1)	57	(17.4)	7.9
			20	#1(V)	30.0	31	(9.4)	62	(18.9)	8.3
				#2(Y)	30.4	31	(9.4)	66	(20.1)	8.2
		Bow	15	#1(V)	31.5	30	(9.1)	56	(17.1)	7.5
				#2(Y)	30.9	30	(9.1)	59	(18.0)	7.5
			20	#1(V)	30.3	30	(9.1)	62	(18.9)	8.2
				#2(Y)	30.1	31	(9.4)	69	(21.0)	8.1

*"Bow" implies 30° off port bow.

**Values may be slightly in error due to transducer wetness.

TABLE 4 - BOW PRESSURE DATA
(PART 1: 20 FOOT NOMINAL SIGNIFICANT WAVE HEIGHT)

Relative Heading*	Ship Speed knots	Location: 60 Foot Waterline at	Bow	Total No. of Impacts	No. of Impacts with Peak Pressure Exceeding 10 lb/in^2 (6.895x10^4 Pa)	30 lb/in^2 (20.685x10^4 Pa)	60 lb/in^2 (41.37x10^4 Pa)	Maximum Peak Pressure lb/in^2 (Pascals x 10^4)	
Head	20	Stem	#1(V)	9	7	1	0	34.0	(23.4)
			#2(Y)	1	1	1	0	30.2	(20.8)
		Station 0	#1(V)	64	0	0	0	< 10	(6.9)
			#2(Y)	35	0	0	0	< 10	(6.9)
		Station 2	#1(V)	7	0	0	0	< 10	(6.9)
			#2(Y)	5	0	0	0	< 10	(6.9)
	25	Stem	#1(V)	155	10	3	2	66.6	(45.9)
			#2(Y)	6	5	3	1	65.7	(45.3)
		Station 0	#1(V)	159	1	0	0	11.2	(7.7)
			#2(Y)	42	3	2	0	36.0	(24.8)
		Station 2	#1(V)	22	0	0	0	< 10	(6.9)
			#2(Y)	17	3	0	0	13.0	(9.0)
Bow	20	Stem	#1(V)	59	2	2	0	37.4	(25.8)
			#2(Y)	2	1	0	0	21.6	(14.9)
		Station 0	#1(V)	88	0	0	0	< 10	(6.9)
			#2(Y)	44	0	0	0	< 10	(6.9)
		Station 2	#1(V)	18	0	0	0	< 10	(6.9)
			#2(Y)	12	0	0	0	< 10	(6.9)
	25	Stem	#1(V)	110	6	2	0	34.0	(23.4)
			#2(Y)	4	2	1	0	31.6	(21.8)
		Station 0	#1(V)	134	1	0	0	11.2	(7.7)
			#2(Y)	73	2	0	0	16.7	(11.5)
		Station 2	#1(V)	26	0	0	0	< 10	(6.9)
			#2(Y)	27	0	0	0	< 10	(6.9)

*"Bow" implies 30° off port bow.

TABLE 4 - BOW PRESSURE DATA
(PART 2: 30 FOOT NOMINAL SIGNIFICANT WAVE HEIGHT)

Relative Heading*	Ship Speed knots	Location: 60 Foot Waterline at	Bow	Total No. of Impacts	No. of Impacts with Peak Pressure Exceeding 10 lb/in^2 (6.895x10^4 Pa)	30 lb/in^2 (20.685x10^4 Pa)	60 lb/in^2 (41.37x10^4 Pa)	Maximum Peak Pressure lb/in^2 (Pascals x 10^4)	
Head	15	Stem	#1(V)	101	15	3	1	66.4	(45.8)
			#2(Y)	18	14	4	1	72.4	(49.9)
		Station 0	#1(V)	83	2	0	0	18.7	(12.9)
			#2(Y)	60	8	0	0	24.6	(17.0)
		Station 2	#1(V)	9	0	0	0	< 10	(6.9)
			#2(Y)	15	2	0	0	14.0	(9.7)
	20	Stem	#1(V)	159	22	6	1	68.5	(47.2)
			#2(Y)	17	10	3	2	87.5	(60.3)
		Station 0	#1(V)	145	4	0	0	25.9	(17.9)
			#2(Y)	59	8	1	0	53.6	(37.0)
		Station 2	#1(V)	31	0	0	0	< 10	(6.9)
			#2(Y)	31	1	0	0	28.5	(19.7)
Bow	15	Stem	#1(V)	77	18	3	0	37.4	(25.8)
			#2(Y)	13	9	2	1	64.8	(44.7)
		Station 0	#1(V)	82	5	0	0	16.7	(11.5)
			#2(Y)	53	8	1	1	66.2	(45.6)
		Station 2	#1(V)	15	1	0	0	10.1	(7.0)
			#2(Y)	19	0	0	0	< 10	(6.9)
	20	Stem	#1(V)	155	28	11	1	64.5	(44.5)
			#2(Y)	28	24	12	1	73.7	(50.8)
		Station 0	#1(V)	152	12	2	0	35.7	(24.6)
			#2(Y)	72	19	2	1	71.1	(49.0)
		Station 2	#1(V)	51	0	0	0	< 10	(6.9)
			#2(Y)	44	2	0	0	15.8	(10.9)

*"Bow" implies 30° off port bow.

TABLE A-1 - BOW PRESSURE TIME CHARACTERISTICS

Location: 60 Foot Waterline at	Bow	Rise Time (seconds)			Duration (seconds)		
		Minimum	Approx. Mode	Maximum	Minimum	Approx. Mode	Maximum
Stem	#1(V)	0.05	0.33	0.60	0.45	1.3	1.96
	#2(Y)	0.03	0.12	0.45	0.26	0.7	1.67
Station 0	#1(V)	0.03	0.07	0.24	0.22	0.4	0.68
	#2(Y)	0.05	0.11	0.24	0.15	0.3	0.68
Station 2	#1(V)*						
	#2(Y)	0.08	0.15	0.21	0.14	0.3	0.41

*p_p > 10 lb/in^2 (6.895 x 10^4 pascals) for only one event.
Then t_0 = 0.14 sec and t_1 = 0.41 sec.

TABLE A-2 - SUMMARY OF BOW PRESSURE PROBABILITY LEVELS

Relative Heading*	Loction: 60 Foot Waterline at	Bow	Percentage Probability of Exceeding 50 lb/in^2 (34.475×10^4 Pa)	Percentage Probability of Exceeding 100 lb/in^2 (6.895×10^5 Pa)
Head	Stem	#1(V)	10.0	0.5
		#2(Y)	16.5	2.6
	Station 0	#1(V)	< 0.1	< 0.1
		#2(Y)	3.2	< 0.1
Bow	Stem	#1(V)	20.0	1.6
		#2(Y)	19.0	1.5
	Station 0	#1(V)	2.5	< 0.1
		#2(Y)	10.0	0.6

*"Bow" implies 30° off port bow.

TABLE A-3 - VERTICAL SLOPE PARAMETERS

Gage Location	Bow	Slope, θ_x deg	cos θ_x
60-S	#1(V)	49	0.65
	#2(Y)	49	0.65
60-0	#1(V)	37	0.79
	#2(Y)	24	0.91
60-2	#1(V)	40	0.76
	#2(Y)	16	0.96
55-3	#1(V)	45	0.71
	#2(Y)	37	0.80
50-0	#1(V)	44	0.72
	#2(Y)	53	0.60
50-2	#1(V)	46	0.69
	#2(Y)	53	0.60

DTNSRDC ISSUES THREE TYPES OF REPORTS

1. DTNSRDC REPORTS, A FORMAL SERIES, CONTAIN INFORMATION OF PERMANENT TECHNICAL VALUE. THEY CARRY A CONSECUTIVE NUMERICAL IDENTIFICATION REGARDLESS OF THEIR CLASSIFICATION OR THE ORIGINATING DEPARTMENT.

2. *DEPARTMENTAL REPORTS, A SEMIFORMAL SERIES, CONTAIN INFORMATION OF A PRELIM*INARY, TEMPORARY, OR PROPRIETARY NATURE OR OF LIMITED INTEREST OR SIGNIFICANCE. THEY CARRY A DEPARTMENTAL ALPHANUMERICAL IDENTIFICATION.

3. TECHNICAL MEMORANDA, AN INFORMAL SERIES, CONTAIN TECHNICAL DOCUMENTATION OF LIMITED USE AND INTEREST. THEY ARE PRIMARILY WORKING PAPERS INTENDED FOR INTERNAL USE. THEY CARRY AN IDENTIFYING NUMBER WHICH INDICATES THEIR TYPE AND THE NUMERICAL CODE OF THE ORIGINATING DEPARTMENT. ANY DISTRIBUTION OUTSIDE DTNSRDC *MUST BE APPROVED BY THE HEAD OF THE ORIGINATING DEPARTMENT ON A CASE-BY-CASE* BASIS.